ELSEVIER

Journal of Nuclear Materials 313–316 (2003) 588–594

journal of nuclear materials

www.elsevier.com/locate/jnucmat

Modeling of global particle balance in steady-state magnetic fusion devices – Analysis of the recent data from the TRIAM-1M tokamak

Yoshi Hirooka [a,*], Mizuki Sakamoto [b], The TRIAM group [b]

[a] National Institute for Fusion Science, 322-6, Oroshi-cho, Toki 509-52, Japan
[b] Advanced Fusion Research Center, RIAM, Kyushu University 87 Kasuga, Fukuoka 816-8580, Japan

Abstract

Global particle balance analysis has been conducted to interpret the data from TRIAM-1M experiments, using a zero-dimension four-reservoir model to calculate the particle inventories in the core plasma, SOL region, gas phase, and wall materials. Two cases have been examined: a relatively short pulse (~30 s) but high density (~10^{19} 1/m^3) LHCD discharge at 8.2 GHz; and a long pulse (~4000 s) but low density (~10^{18} 1/m^3) LHCD discharge at 2.45 GHz. Model calculations have reproduced well the core and SOL plasma densities. Also, the observed wall pumping effects have been analyzed by this model. Measured and model prediction on the wall pumping rate are 4×10^{17} and 4.4×10^{17} 1/m^2/s at 8.2 GHz, and 1.5×10^{16} and 1.8×10^{16} 1/m^2/s at 2.45 GHz, respectively, both relatively good agreements. Also, a parameter sensitivity check has been conducted, and modeling results clearly indicate that the steady state core plasma density decreases with increasing the codeposition probability.

PACS: 52.40.H
Keywords: Wall recycling; Particle balance modeling; Steady state fusion reactors; Wall pumping; Hydrogen recycling; Plasma-wall interactions

1. Introduction

Over the past decade most of the 'sub-critical, i.e., $Q < 1$' fusion experiments have been successfully conducted using large tokamaks such as TFTR and JET, and the construction of ITER (for the International Thermonuclear Experimental Reactor), intended to exceed the energy breakeven, is currently under discussion in the community. Because ITER is planned to be operated in the long pulse mode, the duration of which, however, is limited to 300–500 s [1], due to the Ohmic heating capacity. Interestingly in this regard, recent operation experiences with the TRIAM-1M tokamak have demonstrated that it often takes hours of continuous plasma interactions for wall components to reach thermal equilibria [2]. Therefore, one predicts that the ITER pulse length is not probably long enough for all the in-vessel components to reach steady state temperatures, in which case gas recycling dynamics unavoidably affect edge characteristics and hence the core plasma performance throughout the course of pulse duration. Clearly, not all the technical issues associated with steady state operation will be resolved by ITER even if it went successfully.

Among these remaining issues, particle balance and its control are critical in achieving true steady

* Corresponding author. Tel.: +81-572 58 2256; fax: +81-572 58 2628.
E-mail address: hirooka@nifs.ac.jp (Y. Hirooka).

0022-3115/03/$ - see front matter
PII: S0022-3115(02)01419-8

state because they can determine the overall reactor performance as to fuel economy and related on-site radiation safety, lifetime of the plasma-facing components and core plasma stability. Though it has not been clearly addressed until now, well-regulated fusion power generation probably requires solomonic control over particle balance because local plasma behavior is not quite at steady state due to the facts that core fueling is discontinuous, if it is done by pellet injection, and that edge energy bursts due to ELMs is generally high-frequency but not truly continuous, etc. Responses to these operation 'kick-backs' from plasma-facing components are yet to be explored in ITER and fusion devices beyond it.

In our previous work a zero-dimension, but four-reservoir (core, SOL, gas, wall) particle balance model was constructed and successfully applied to analyze the transient density decay phenomena observed in LHD during NBI heating [3]. Modeling results also pointed out that in an ITER-size reactor wall pumping to maintain particle recycling below 100% would be essential in controlling the particle balance at steady state although the build-up of tritium is a safety issue to be concerned separately.

In the present work this particle balance model has been modified to incorporate some of the key features of plasma–surface interactions in TRIAM-1M and then applied to interpret the wall pumping effects observed in long-pulse limiter discharges, as long as 4000 s, all heated by LHCD [4]. The significance of wall pumping as to particle balance is again pointed out even in a small-size device.

2. Particle balance model

In this section the specifics of plasma–surface interactions in the TRIAM-1M tokamak are briefly described, and implemented in the model equations which then will be modified from the last version applied for the LHD data analysis [3]. Recent measurements at TRIAM-1M have indicated that the core as well as SOL plasmas lose particles with high energies due to charge-exchange reactions [4]. This is illustrated in Fig. 1, together with other key particle exchange flows among the reservoirs: core, SOL, gas phase and wall, hypothesized in the model. Due to these charge exchange neutrals with high energies, the entire in-vessel wall is believed to be subjected to rather high-yield sputtering. Also, the limiter surface will be bombarded with confinement loss ions from the SOL region. All these particle bombardment events will lead to materials erosion which then is followed by the co-deposition with hydrogen. Taking into account these features, the resultant particle balance equations are:

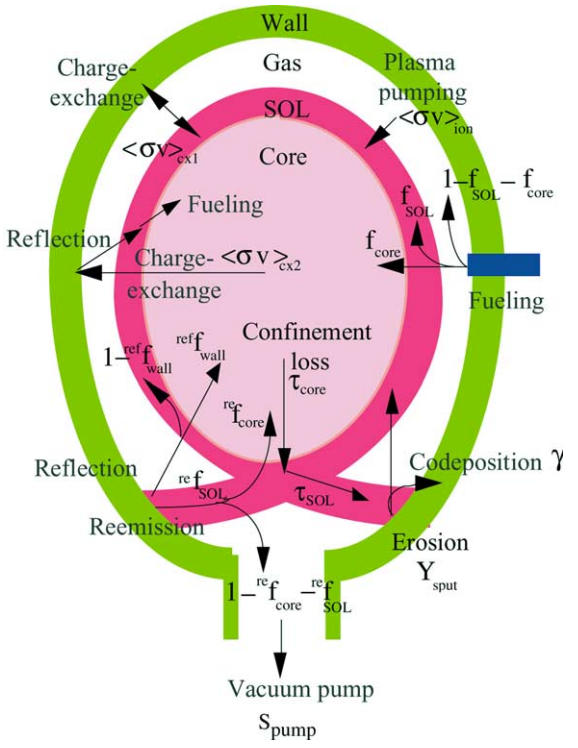

Fig. 1. A schematic diagram of particle exchange flows among the four reservoirs: core, SOL, gas and wall of a magnetic fusion reactor, hypothesized in the model.

$$\frac{dN_{core}}{dt} = -\frac{N_{core}}{\tau_{core}} + \alpha_1 \frac{\langle\sigma v\rangle_{cx1}}{2V_{gas}} N_{gas} N_{SOL} - \alpha_2 \frac{\langle\sigma v\rangle_{cx2}}{V_{gas}} N_{gas} N_{core} + \left(\frac{N_{SOL}}{\tau_{SOL}} + \alpha_1 \frac{\langle\sigma v\rangle_{cx1}}{2V_{gas}} N_{gas} N_{SOL} + \alpha_2 \frac{\langle\sigma v\rangle_{cx2}}{V_{gas}} N_{gas} N_{core} \right) (R_e^{re} f_{core} + R_{ef}^{ref} f_{core}) + f_{core} \Phi_{ext}, \quad (1)$$

$$\frac{dN_{SOL}}{dt} = -\frac{N_{SOL}}{\tau_{SOL}} + \frac{N_{core}}{\tau_{core}} - \alpha_1 \frac{\langle\sigma v\rangle_{cx1}}{V_{gas}} N_{gas} N_{SOL} + \beta \frac{\langle\sigma v\rangle_{ion}}{V_{SOL}} N_{gas} N_{SOL} + \left(\frac{N_{SOL}}{\tau_{SOL}} + \alpha_1 \frac{\langle\sigma v\rangle_{cx1}}{2V_{gas}} N_{gas} N_{SOL} + \alpha_2 \frac{\langle\sigma v\rangle_{cx2}}{V_{gas}} N_{gas} N_{core} \right) \{ R_e^{re} f_{SOL} + R_{ef} (1 - {}^{ref} f_{core}) \} + f_{SOL} \Phi_{ext}, \quad (2)$$

$$\frac{dN_{gas}}{dt} = -S_{pump}N_{gas} - \beta\frac{\langle\sigma v\rangle_{ion}}{V_{SOL}}N_{gas}N_{SOL} + \left(\frac{N_{SOL}}{\tau_{SOL}} + \alpha_1\frac{\langle\sigma v\rangle_{cx1}}{2V_{gas}}N_{gas}N_{SOL} + \alpha_2\frac{\langle\sigma v\rangle_{cx2}}{V_{gas}}N_{gas}N_{core}\right)(R_e(1 - {}^{re}f_{SOL} - {}^{re}f_{core}) - \gamma\left(Y_{sput}\frac{N_{SOL}}{\tau_{SOL}} + Y_{sput\text{-}1}\alpha_1\frac{\langle\sigma v\rangle_{cx1}}{2V_{gas}}N_{gas}N_{SOL} + Y_{sput\text{-}2}\alpha_2\frac{\langle\sigma v\rangle_{cx2}}{V_{gas}}N_{gas}N_{core}\right) + (1 - f_{core} - f_{SOL})\Phi_{ext}, \quad (3)$$

$$\frac{dN_{wall}}{dt} = \left(\frac{N_{SOL}}{\tau_{SOL}} + \alpha_1\frac{\langle\sigma v\rangle_{cx1}}{2V_{gas}}N_{gas}N_{SOL} + \alpha_2\frac{\langle\sigma v\rangle_{cx2}}{V_{gas}}N_{gas}N_{core}\right)(1 - R_e - R_{ef}) + \gamma\left(Y_{sput}\frac{N_{SOL}}{\tau_{SOL}} + Y_{sput\text{-}1}\alpha_1\frac{\langle\sigma v\rangle_{cx1}}{2V_{gas}}N_{gas}N_{SOL} + Y_{sput\text{-}2}\alpha_2\frac{\langle\sigma v\rangle_{cx2}}{V_{gas}}N_{gas}N_{core}\right), \quad (4)$$

where N_{core}, N_{SOL}, N_{gas}, N_{wall} are the particle inventories in the core, SOL, gas, and wall, respectively, α_1, α_2, β, are adjusting parameters to express degrees of separation between the SOL and gas regions, for example, in the case of closed divertor, although they are set as $\alpha_1 = \alpha_2 = \beta = 1$ in the present work, γ is the co-deposition probability, R_e is the reemission coefficient, and R_{ef} is the reflection coefficient. All other symbols have their usual meanings. Also, it is important to note that the overall reactor particle balance equation, which can be obtained from the summation of Eqs. (1)–(4) is given as:

$$\frac{dN_{overall}}{dt} = -S_{pump}N_{gas} + \Phi_{ext}. \quad (5)$$

Notice that the overall particle balance equation is extremely simple. This is because individual inflows and outflows of particles among these reservoirs cancel each other.

3. Results and discussion

3.1. Comparison between the previous and present models

In the previous report [4], the hydrogen recycling data from TRIAM-1M experiments were analyzed using the zero-dimension, single-reservoir particle balance model featured with the following equation [4]:

$$\frac{dN_e}{dt} = \eta S_g - (1 - R)\frac{N_e}{\tau_p}, \quad (6)$$

where η is the fueling efficiency, S_g is the fueling rate and the rest of symbols have their usual meanings. Note that the term, R, may be considered as 'total' recycling coefficient, which composes of contributions of reemitted molecules and reflected atoms to the core fueling. Total recycling coefficients were then calculated, using the data from line-averaged plasma density and H_α light intensity measurements conducted for 2.45 and 8.2 GHz LHCD-heated plasmas, and are reproduced in Fig. 2 for the sake of modeling in the present work. These curves are fitted with the following equations:

$$R_{8.2\ GHz}(t) = 0.999 - 0.0074567\exp(-t/10.986[s]) - 0.4154\exp(-t/0.3993[s]), \quad (7)$$

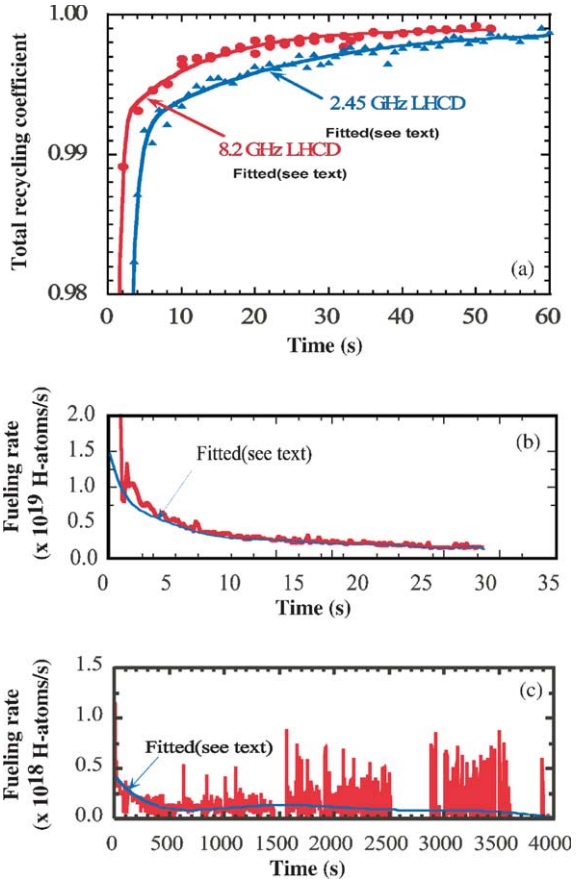

Fig. 2. Experimental data from the TRIAM-1M tokamak: reproduced data from Ref. [2] and fitted curves for the model calculation in the present work: (a) total recycling coefficients for shot#66276 and shot#57379, (b) external fueling for the 8.2 GHz LHCD discharge (shot#66276) and (c) external fueling for the 2.45 GHz LHCD discharge (shot#57379).

Table 1
Parameters used in the modeling analysis for the TRIAM-1M data

Parameters	8.2 GHz LHCD	2.45 GHz LHCD
V_{core}	2×10^{-1} m^3	2×10^{-1} m^3
V_{SOL}	2×10^{-1} m^3	2×10^{-1} m^3
V_{gas}	6×10^{-1} m^3	6×10^{-1} m^3
τ_{core}	0.01 s	0.02 s
τ_{SOL}	0.0002 s	0.0004 s
$R_e(t)$	see text	see text
$R_{ef}(t)$	0.5 (at $E^* = 300$ eV)	0.45 ($E = 600$ eV)
$\Phi_{ext}(t)$	see text	see text
f_{core}	0.2	0.2
${}^{re}f_{core}$	0.8	0.8
f_{SOL}, ${}^{re}f_{SOL}$	0.198	0.196
${}^{ref}f_{core}$	0.7	0.7
${}^{ref}f_{SOL}$	0	0
$\langle\sigma v\rangle_{cx1}$	3×10^{-14} m^3/s	3×10^{-14} m^3/s
$\langle\sigma v\rangle_{cx2}$	7×10^{-14} m^3/s	7×10^{-14} m^3/s
$\langle\sigma v\rangle_{ion}$	2×10^{-14} m^3/s	2×10^{-14} m^3/s
S_{pmp}	0.55 m^3/s	0.55 m^3/s
Y_{sput}[a]	0 ($E^a = 50$ eV)	0 ($E = 50$ eV)
Y_{sput-1}	0 ($E = 10$ eV)	0 ($E = 10$ eV)
Y_{sput-2}	0.0005 (at $E = 300$ eV)	0.0038 ($E = 600$ eV)
γ	0.3	0.3

[a] Y_{sput}, Y_{sput-1}, Y_{sput-2} are the sputtering yields of molybdenum due to the SOL-confinement loss ions, charge-exchange neutrals from the SOL region and charge-exchange particles from the core plasma, respectively. The term, E, is the particle bombarding energy. The electron temperature, T_e, in the SOL region is typically of the order of 10 eV in TRIAM-1M, so that the bombarding energy of SOL-confinement loss ions is assumed to be given by $5kT_e \sim 60$ eV. Under these conditions, Y_{sput} and Y_{sput-1} are considered to be negligible even as ion energies have the Maxwellian distribution.

$$R_{2.45\ GHz}(t) = 0.998 - 0.0089708\exp(-t/12.721[s]) - 0.53903\exp(-t/0.85603[s]), \quad (8)$$

where t is the time, and fitting has been done, assuming that $R(0) = R_{ef}$ (see Table 1).

In order that the present model can be applied to analyze the TRIAM-1M data, the total recycling coefficient in Eq. (6) needs to be related to the recycling and fueling constants that appear in Eqs. (1)–(4). This can be done by adding Eq. (1) to Eq. (2) to compare the result with Eq. (6). This comparison leads to the following relation:

$$R = R_e({}^{re}f_{core} + {}^{re}f_{SOL}) + R_{ef}. \quad (9)$$

From Eqs. (7)–(9), the reemission coefficient, R_e, is estimated as needed during the course of computation, where the reflection coefficient, R_{ef}, is calculated separately, using the TRIM-SP code [5].

3.2. Modeling details

Key parameters used for the present model are summarized in Table 1. As is always the case with particle balance modeling of this kind, not all the parameters are independently measurable. However, uncertainties are within a factor of 2–3 on these parameters, which probably is the best one can expect.

As indicated by Eqs. (3) and (4), hydrogen co-deposition can directly affect the particle balance behavior. Therefore, the sputtering yield and co-deposition probability must be estimated as accurately as possible, taking into account the actual wall characteristics. Interestingly, spectroscopic data taken at TRIAM-1M have indicated that the major metallic impurity is not iron from the stainless steel first wall, but molybdenum, presumably eroded from the limiter and divertor [6]. One predicts that generally, once they are eroded from any plasma-facing components, materials will then be redeposited over the surface, forming coatings with a variety of thicknesses. In fact, deposition probe analysis has indicated that molybdenum is the major metallic impurity [7]. In the present work, therefore, we assume that the entire wall surface is coated with molybdenum regardless of substrate materials.

As mentioned earlier, in TRIAM-1M, the core plasma loses particles due to charge-exchange reactions as well as confinement losses. Consistently, measured neutral particle energies range up to the core plasma temperatures, which are typically ~300 and ~600 eV for the 8.2 and 2.45 GHz LHCD plasmas, respectively. These energies are used for sputtering yield and reflection coefficient calculations in Eqs. (4) and (9). The ion bombarding energy due to particles escaping from the SOL region is generally given by the relation: $E_i = 5kT_e$ where k is the Boltzman constant and T_e is the electron temperature. Because the edge electron temperature is around 20 eV in these plasma discharges, there is virtually no sputtering of molybdenum by hydrogen, the threshold energy of which is calculated to be 275 eV using Yamamura's formula [8]. Generally, one assumes little hydrogen codeposition with molybdenum. However, the recent materials analysis data [7] have indicated that in the presence of oxygen impurities, hydrogen co-deposition in metallic co-deposits can be as significant as in carbon co-deposits. In the present model, therefore, the hydrogen codeposition characteristics are assumed to be such that $\gamma = 0.3$.

For the external fueling by gas-puff, experimental data are fitted with the following equations:

$$F_{8.2\ GHz}(t) = 2.4902 \times 10^{19} - 1.3654 \times 10^{19}t + 4.4882 \times 10^{18}t^2 - 8.441 \times 10^{17}t^3 + 9.4903 \times 10^{16}t^4 - 6.5948 \times 10^{15}t^5 + 2.854 \times 10^{14}t^6 - 7.4826 \times 10^{12}t^7 + 1.0869 \times 10^{11}t^8 - 6.708 \times 10^{8}t^9, \quad (10)$$

$$F_{2.45\ \mathrm{GHz}}(t) = 4.503 \times 10^{17} - 1.3724 \times 10^{15} t + 1.927 \times 10^{12} t^2 - 1.1588 \times 10^{9} t^3 + 2.9156 \times 10^{5} t^4 - 8.8229 t^5 - 0.0080435 t^6 + 9.6099 \times 10^{-7} t^7, \quad (11)$$

where in the case of 2.45 GHz, the gas puffing rate fluctuates so severely, exhibiting several times of complete shut-off, that an averaging curve is employed for simplicity, as illustrated in Fig. 2(c).

The core fueling efficiency is set at 20% for gas-puffed hydrogen molecules whereas, due to the fact that the gap between the first wall and the last closed flux surface in TRIAM-1M is only 1–2 cm, we assume that the re-fueling efficiency of reemitted molecules is 80%. As to wall-reflected atoms, the fueling efficiency is assumed to be 70% for the core, but 0% for the SOL region because of their relatively high energies.

From separate measurements [6], the particle confinement time for the core plasma has been found to decrease from about 20 to 10 ms while the core density changes from about 1.5×10^{18} to 3×10^{18} 1/m^3 [6]. The confinement time for the SOL region is assumed to be 1/50 of that for the core in this modeling.

3.3. Modeling results and comparison with experimental data

Using these equations and data listed in Table 1, zero-dimension, four-reservoir particle balance modeling has been performed and the results are presented in Figs. 3 and 4, together with the corresponding experimental data for comparison.

As can be seen in Fig. 3(a) and (c), the core plasma density during the steady state, attained after about $t = 10$ s in the case of 8.2 GHz (shot#66276), has been nicely reproduced by the model. Similar agreement has been obtained for the SOL plasma density, although the data are not shown here. Also, one finds agreement between the experimental data and modeling results in Fig. 4(a) and (c) in the case of 2.45 GHz LHCD (shot#57379). Model predictions on steady-state neutral pressure for these plasma discharges are 5×10^{-6} Torr (taken at $t = 20$ s) for shot#66276 and 6×10^{-7} Torr (taken at $t = 3000$ s) for shot#57379, which one finds are in relatively good agreement with 3.1×10^{-6} and 9.2×10^{-7} Torr, respectively, measured nearby the turbo-molecular pump.

Turning to the wall pumping effect, shown in Fig. 3(b) are the numbers of particles estimated from external fueling and active pumping in the case of 8.2 GHz LHCD (shot#66276), the difference between which is considered to be due to passive pumping by the wall. The time-averaged wall pumping rate calculated from these data is 4×10^{16} H/m^2/s, and the corresponding value from modeling is 4.4×10^{16} H/m^2/s, shown in Fig. 3(d), which is rather good agreement. From the data shown in Fig. 4(b) and (d), the wall pumping speed evaluated from the experimental data is 1.5×10^{16} H/m^2/s, and the modeling result is 1.8×10^{13} H/m^2/s, again, good agreement.

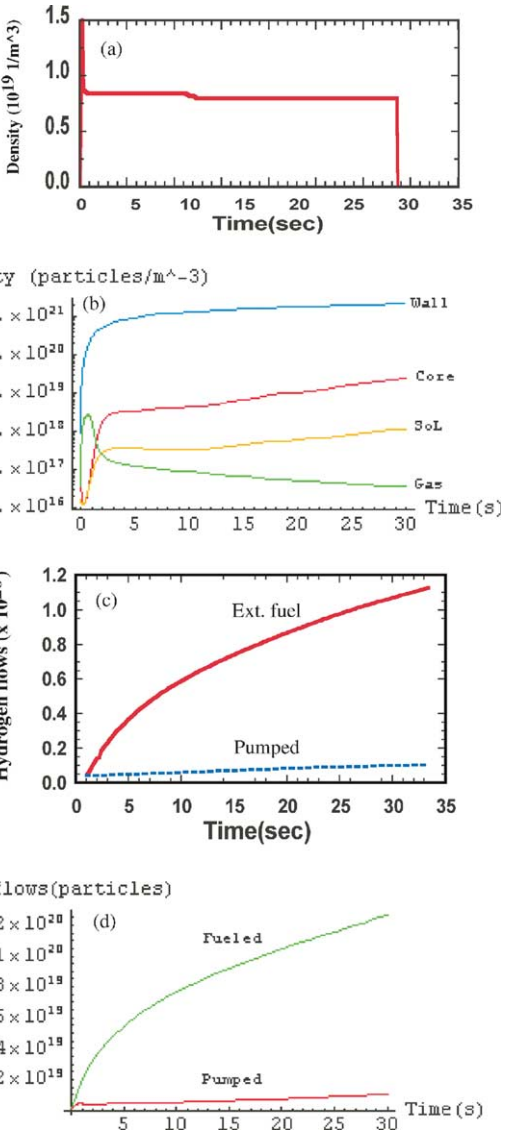

Fig. 3. A comparison between the experimental data and modeling results: (a) line-averaged density during the 8.2 GHz LHCD discharge (shot#66276), (b) densities in the four reservoirs, (c) hydrogen flows due to external fueling and pumping and (d) modeling results for the hydrogen flows due to external fueling and pumping.

3.4. Parameter sensitivity check

For the sake of parameter sensitivity check, the co-deposition probability has been varied from 0 to 1, al-

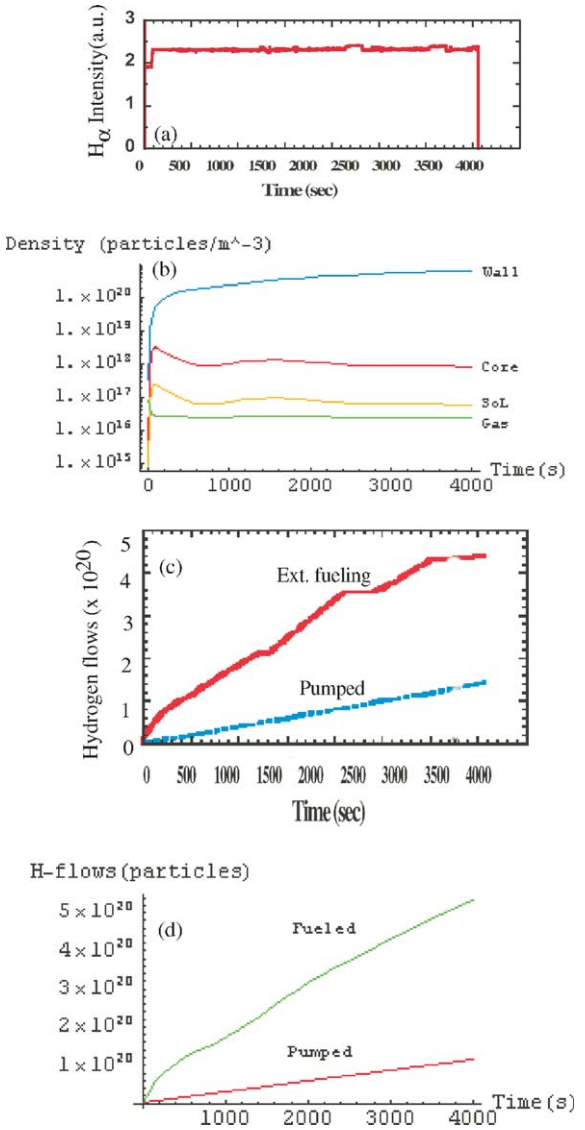

Fig. 4. A comparison between the experimental data and modeling results: (a) line-averaged density during the 2.45 GHz LHCD discharge (shot#57379), (b) densities in the four reservoirs, (c) hydrogen flows due to external fueling and pumping and (d) modeling results for the hydrogen flows due to external fueling and pumping.

though it seems to be highly unlikely to exceed 0.5. Here, the co-deposition probability of unity means one hydrogen atom per redeposited atom. The results are presented in Fig. 5, showing the steady state core and SOL plasma densities at $t = 3000$ s employing parameters used for the 2.45 GHz LHCD discharge simulation. One finds that the plasma density decreases rather rapidly as the co-deposition probability increases up to around 0.5. However, at codeposition probabilities

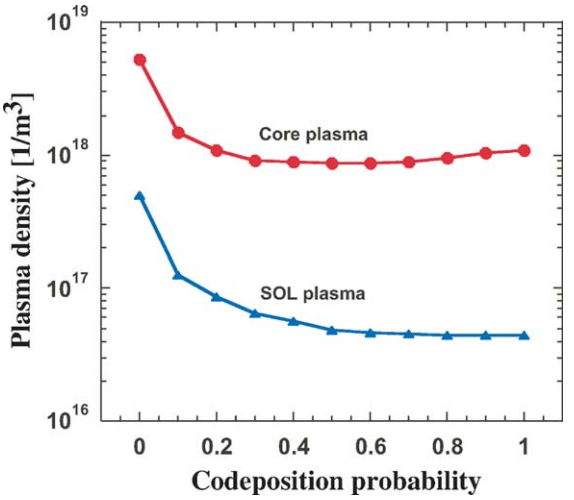

Fig. 5. Core and SOL plasma densities predicted as a function of hydrogen codeposition probability under the identical modeling conditions to those employed in the case of 2.45 GHz LHCD (shot#57379).

above this level, one finds little change for the core and SOL plasma densities, the physics of which is not clear yet. Therefore, because virtually they determine the wall recycling coefficient, hydrogen co-deposition characteristics are considered to be influential on the overall particle balance of a reactor system. Interestingly, the convergence of numerical solutions for Eqs. (1)–(4) depends much more strongly on the fitting formula for hydrogen recycling curves such as those given by Eqs. (7) and (8) than the co-deposition probability. This is presumably because in the present work the sputtering yield of molybdenum is relatively small, and hence the co-deposition probability does not strongly affect the actual hydrogen recycling.

4. Conclusion

The model applied for the analysis of TRIAMI-1M data is relatively simple from the physics point of view, but has been proven to be rather flexible in analyzing the wall recycling data from a variety of systems, including LHD, an ITER-size device, and a small device such as TRIAM-1M. The key in this kind of modeling is to choose the right set of parameters that reflect the physics in these devices appropriately, even as they are not quite precisely correct. Based on the validation of this model, the codeposition parameter sensitivity check has been conducted and results have indicated that wall pumping characteristics can directly affect the core plasma density and hence the overall system particle balance. In other words, as has often been pointed out [3], the wall

pumping is probably necessary from the particle control point of view although one has to be aware of the safety hazard due to tritium build-up.

References

[1] R. Aymar, Fusion Eng. Des. 55 (2002) 107.
[2] M. Sakamoto and the TRIAM group, Journal of Plasma and Fusion Research Series, vol. 5, in press.
[3] Y. Hirooka et al., J. Nucl. Mater. 290–293 (2001) 423.
[4] M. Sakamoto et al., Nucl. Fusion 42 (2002) 165.
[5] J.P. Biersack, W. Ecstein, Appl. Phys. A 34 (1984) 73.
[6] M. Sakamoto, private communication.
[7] T. Hirai et al., J. Nucl. Mater. 283–287 (2000) 1177.
[8] N. Matsunami et al., At. Data Nucl. Data Tables 31 (1984) 1.